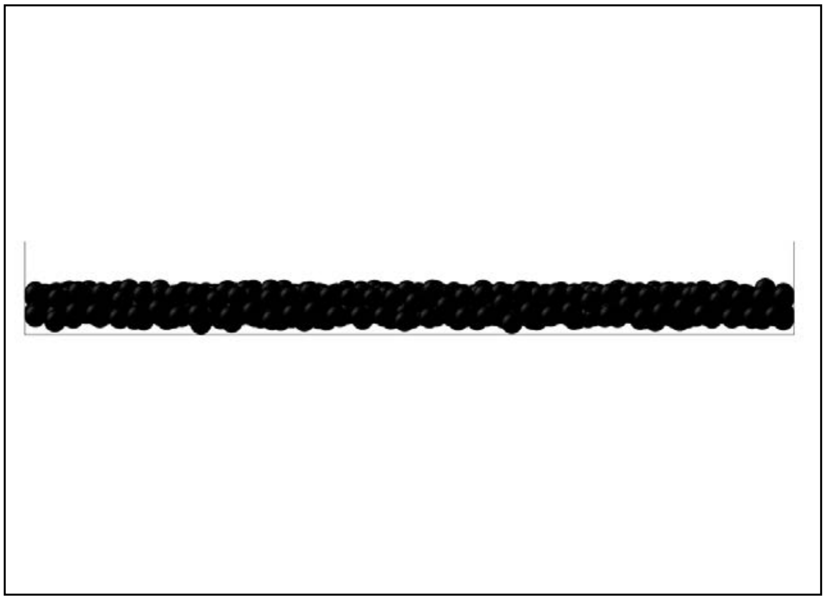

Numerical Experiments in Multiphase CFD: Artificial Levitation of a Very Shallow Fluidized Bed in CFD-DEM

5 October 2018

Office of Fossil Energy

NETL-TRS-19-2018

Disclaimer

Cover Illustration: Particles levitating above a gas inlet.

Suggested Citation: Fullmer, W. D.; Xu, Y.; Dietiker, J.-F. *Numerical Experiments in Multiphase CFD: Artificial Levitation of a Very Shallow Fluidized Bed in CFD-DEM*; NETL-TRS-19-2018; NETL Technical Report Series; U.S. Department of Energy, National Energy Technology Laboratory: Morgantown, WV, 2018; p 20. DOI: 10.18141/1476713.

An electronic version of this report can be found at:

http://netl.doe.gov/research/on-site-research/publications/featured-technical-reports

Numerical Experiments in Multiphase CFD:
Artificial Levitation of a Very Shallow Fluidized Bed in CFD-DEM

William D. Fullmer[1], Yupeng Xu[2], Jean-François Dietiker[2]

[1]U.S. Department of Energy, National Energy Technology Laboratory, AECOM, 3610 Collins Ferry Road, Morgantown, WV 26507

[2]U.S. Department of Energy, National Energy Technology Laboratory, West Virginia University Research Corporation, 3610 Collins Ferry Road, Morgantown, WV

NETL-TRS-19-2018

5 October 2018

NETL Contacts:
Jordan Musser, Principal Investigator
Jonathan Lekse, Technical Portfolio Lead
Bryan Morreale, Executive Director, Research & Innovation Center

This page intentionally left blank.

Table of Contents

This page intentionally left blank.

List of Figures

List of Tables

This page intentionally left blank.

Acronyms, Abbreviations, and Symbols

Term	Description
2-D	Two-dimensional
CFD	Computational fluid dynamics
DEM	Discrete element model
DMP	Distributed memory parallelism
DPVM	Divided particle volume method
HDPE	High-density polyethylene
NETL	National Energy Technology Laboratory's
Latin	
d	Diameter
e	Restitution coefficient
k	Spring constant
L	System size
N	Number of particles or CFD cells
p	Pressure
U	Gas superficial velocity
Greek	
Δ	CFD grid size
δ	Difference or filter width
ρ	Density
μ	Viscosity or friction coefficient
Subscripts	
*	Non-dimensional
f	Filter
g	Gas-phase
j	CFD grid y-coordinate index
mf	Minimum fluidization
n	Normal (direction)
O	Outlet
p, pp, pw	Particle-phase, particle-particle, particle-wall
WY	Wen and Yu (1966) correlation
x, y, z	Cartesian coordinates

Acknowledgments

This work was completed as part of National Energy Technology Laboratory (NETL) research for the U.S. Department of Energy's (DOE) Advanced Reaction Systems (ARS) Program. This technical effort was performed in support of the National Energy Technology Laboratory's ongoing research under the RES contract DE-FE0004000.

ABSTRACT

This report investigates the fluidization of a very shallow bed using computational fluid dynamics-discrete element model (CFD-DEM). Under certain conditions, the thin layer will artificially levitate above the inlet in a stable, static configuration. It was determined that the levitation is caused by a balance in particle forces with particles in the lower half of the layer experiencing a different pressure gradient than particles in the upper half. The difference arises from the pressure profile itself (namely a local minimum above the layer) and differences in the numerical differentiation scheme between general and wall adjacent cells. It was determined that this behavior is not caused by a deficiency in the numerical method or a bug in the specific implementation. Instead, this study suggests using a high-resolution grid when simulating very shallow fluidized beds that would fit within one or two rows of cells using a typical CFD-DEM discretization.

1. PROBLEM STATEMENT

Recently, a computational fluid dynamics-discrete element model (CFD-DEM) simulation was set up by a coauthor (YX) for biomass gasification in a small fluidized bed. The problem size, specifically the particle count, was significantly reduced for testing purposes. The resulting bed, however, displayed strange hydrodynamics—even when the chemical reactions were removed. Namely, the thin layer of particles appeared to float or levitate above the distributor. Further, the grid resolution was found to be strongly linked to this problem with a finer resolution giving a more realistic behavior. This report studies the floating layer problem to determine if there is a correction or improvement that can be made to prevent this behavior in a typical CFD-DEM scheme.

2. MODEL DESCRIPTION

A hypothetical pseudo-two-dimensional “2-D”' (i.e., thin in the depth dimension) bed geometry was set up as described in Table 1. The bed material is similar to high-density polyethylene (HDPE) particles in air, hypothetical properties also provided in Table 1. With these material properties, the Wen and Yu correlation for minimum fluidization (Wen and Yu, 1966) gives U_{mf}^{WY} ~ 0.26 m/s. Except where noted, the superficial gas velocity is set to U = 1 m/s at the inlet plane (y = 0). The left and right walls (x = 0 and L_x, respectively) are no slip boundaries for the gas-phase while the front and back walls (z = 0 and L_z, respectively) are treated as free slip. A pressure outflow boundary is specified at the outlet ($y = L_y$). The bed is initialized at rest with 864 randomly distributed particles which corresponds to two perfectly arranged layers. Simulations were run for a period of 1 s which is long enough to observe what type of behavior will be displayed by the bed at a given grid resolution.

Table 1: Simulation Parameters

Bed Properties		
Width	L_x	36 mm
Height	L_y	72 mm
Depth	L_z	12 mm
Grid	Δ^*	variable
Particle Properties		
Number	N_p	864
Diameter	d_p	1 mm
Density	ρ_p	1,000 kg/m^3
Collision Properties		
Restitution Coefficient	e_{pp}, e_{pw}	0.95
Friction Coefficient	μ_{pp}, μ_{pw}	0.10
Spring Stiffness	k_n	440
Fluid Properties		
Density	ρ_g	1.2 (kg/m^3)
Viscosity	μ_g	1.8e-5 (Pa-s)

The National Energy Technology Laboratory’s (NETL) open-source MFiX code (mfix.netl.doe.gov), Release 2016.1, is used to study the levitating layer. The complete CFD-DEM governing equations have been reported previously by Garg et al., (2012; 2012b). In general, MFiX couples a finite volume CFD solver with a soft-sphere DEM model. A SIMPLE-type pressure-velocity coupling is used with a residual tolerance of 1e-3 (NORM_G = 0 normalization). Gas velocity components are stored at cell faces staggered from the pressure and concentration stored at cell centers. The SMART flux-limiter is applied for variable extrapolation (Waterson and Deconinck, 2007). Euler time stepping is used for both CFD and DEM advancement. The CFD timestep is variable with a maximum of one collision duration. The maximum DEM timestep is one twentieth of the collision duration. A linear spring dashpot collision model is applied. The uniform (square) divided particle volume method (DPVM) is used for the discrete-continuum transfer. The width of the square DPVM is set to 1.5 d_p. Finally, interfacial momentum transfer is closed with the steady drag model of Gidaspow (GIDASPOW_BLEND) (Ding and Gidaspow, 1990; Lathouwers and Bellan, 2001).

3. RESULTS

To study the effect of resolution on the fluidization behavior, several different CFD grids are used ranging from $\Delta^* = 4$ to 1, where $\Delta^* = (L_x \times L_y \times L_z / N_{xyz})^{1/3}/d_p$ is the grid spacing nondimensionalized by the particle diameter and $N_{xyz} = N_x \times N_y \times N_z$ are the total number of CFD cells. The state of the particles at $t = 1$ s is shown in Figure 1 colored by velocity magnitude. For the baseline superficial velocity of $U = 1$ m/s, the resolution dependent dynamics are summarized below.

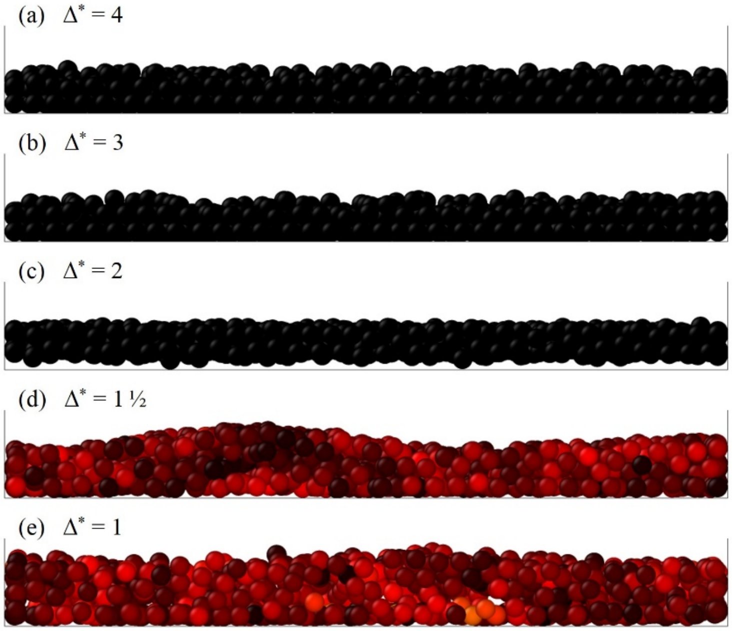

Figure 1: Side view of particle configuration at *t* = 1 s colored by instantaneous particle velocity magnitude ranging from 0 (black) to *U* (white).

- **(Δ^* = 3 and 4)** On the two coarsest discretizations studied here, the thin layer fails to fluidize at all. The particles fall from their random initial positions to the inlet and rest on the bottom of the domain for roughly half of the simulation time. Figure 1(a, b) shows that the 864 particles collapse into roughly two and a half packed layers. The thin layer is static even though it is being fluidized at nearly four U_{mf}^{WY}. The (primary) reason for this static condition is the under-prediction of the void fraction. Assuming all particles are in the lowest row ($j = 1$) of cells, the mean concentration in this row is approximately the inverse of the dimensionless grid size. Therefore, (most) particles experience a concentration of $\phi \sim 1/4$ and 1/3 which may not be realistic for the configurations in Figure 1(a, b), especially for particles in the lowest layer. A secondary consequence of the under-prediction of solids concentration is the under-prediction of the gas-phase pressure gradient which only acts to compound the issue. The pressure profile near the bottom of the bed is shown in Figure 2.
- **(Δ^* = 2)** A grid resolution of $\Delta^* = 2$, for this configuration, provides the “magic” conditions for levitation. In this case, after the particles settle on the bottom, they rise

slowly until the thin layer is no longer supported from below by the inlet and freeze into a nearly static, floating configuration as shown in Figure 1(c). The gas-phase pressure drop in the vicinity of the layer reveals the secret of the levitation. The lowest row (j = 1) of CFD cells likely experience a near realistic concentration as the particles are able to fill one (CFD) row for Δ^* = 2. Indeed, the pressure gradient for Δ^* = 2 in Figure 2 is in fairly good agreement with the higher resolution profiles. However, only particles in the bottom row experience the pressure gradient given by the difference of $\delta p_{g,j=1} \sim p_{g,j=2} - p_{g,j=1}$. More specifically, the pressure gradient must be down-winded from above since pressure is not defined at an inflow boundary condition. The down-winded pressure gradient is sufficient to fluidize the particles which initially causes the layer to rise. However, particles on the top of the layer which reach the second row of cells (j = 2) do not experience the same pressure gradient, taken as a center difference in non-boundary cells. Figure 2 shows that $p_{g,j=3} > p_{g,j=2}$, i.e., there is actually a small region of positive pressure gradient. Consequently, the pressure gradient in the second row is less than that of the first row. Evidentially, the reduced pressure gradient and likely reduced concentration (reduced drag force) is insufficient to fluidize the particles on top, and the layer is split between particles of opposing (vertical) forces creating a relatively stable, static layer of particles levitating around the first and second rows of CFD cells.

- **(Δ^* = 3/2)** As the resolution is increased to Δ^* = 1.5 another odd behavior is displayed. Rather than levitating, as the layer begins to rise in this case a transverse (left to right) wave pattern is formed so that, while the particles are not static, the bed does not fluidize in a typical fashion. Despite the different behaviors, the pressure profiles of Δ^* = 1.5 and Δ^* = 2 are quite similar, demonstrating the relatively sensitive conditions required for levitation.

- **(Δ^* = 1)** Finally, at Δ^* = 1, the thin layer is sufficiently resolved that the (center-differenced) pressure gradient in the second row is equal to the down-winded pressure gradient in the first row. At this resolution, particles on top of the layer reside in the third rows of CFD cells (j = 3). However, this pressure gradient ($\delta p_{g,j=3} \sim p_{g,j=4} - p_{g,j=2}$) is much closer to that experienced in the first row since the index of the local pressure minimum has increased to j = 4. (Note that the actual elevation of the pressure minima has not increased, simply the index.) At this resolution, the thin layer exhibits relatively uniform fluidization, in qualitative agreement with what may be expected under such conditions.

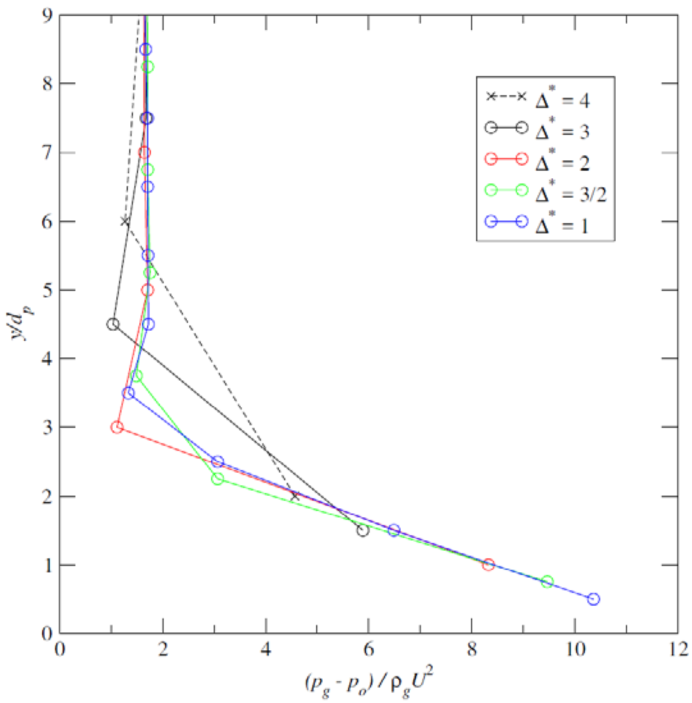

Figure 2: Gas-phase vertical pressure profile averaged over bed width and depth from *t* = 0.5 to 1 s.

A few additional findings of related simulations are summarized below.

- The levitating layer behavior is restricted to very shallow beds. When the particle count is increased ten-fold, the (relatively) deeper bed fluidizes naturally with $\Delta^* = 2$. The reason seems to be that a relatively equal number of particles is needed in the CFD rows resulting in balanced opposing forces. When there are many layers of particles with net positive vertical forces, they simply overwhelm any balance with the layer or two of particles on top of the bed with net negative vertical forces. Indeed, an “unfluidized” layer of particles at the top of all bubbling beds, at least in CFD-DEM, may be quite common.

- The levitating layer behavior is restricted to near-U_{mf} region. If the superficial velocity is increased enough, the thin layer will fluidize even with very poor predictions of volume fraction. For example, $\Delta^* = 4$ fluidizes when the gas inflow velocity set at $U = 3$ m/s. Interestingly, with $\Delta^* = 4$ and $U = 2$ m/s, the system starts to fluidize but the particles became stuck in a levitating layer at the interface of the first and second row of CFD cells. This artificial levitation was even more pronounced than in Figure 1(c) as the elevation of the layer doubled.

- A similar phenomenon was also reported by YX for a bi-dispersed mixture. The superficial velocity was very near U_{mf} of the primary bed material (sand) and above that of the secondary material (biomass). The biomass particles fluidized naturally inside of the sand bed, but, upon segregating and reaching the surface, appeared to float above the surface of the sand bed in a very thin layer (due to the low particle count). It was presumed that the same artificial levitation phenomena was responsible, albeit in a more complicated fashion.

4. CONCLUSIONS/RECOMMENDATIONS

In this case, there does not seem to be anything inherently wrong with either the CFD-DEM method in general nor its specific MFiX implementation. The pressure gradient could perhaps be upwinded, however, this may not have sound physical basis. Rather, if a very shallow bed is actually the problem of interest (which it was not in this case originally—the shallow bed was a consequence of troubleshooting) it is recommended to use a very fine grid in order to resolve the pressure gradient and solids volume fraction of the bed more accurately. Application of a high-resolution grid does require a more complicated particle-grid deposition scheme, however, resolving the entire bed with one or two rows of CFD cells is simply insufficient to study very shallow fluidized beds with CFD-DEM.

5. FOLLOW-UP: HIGH-RESOLUTION GAUSSIAN KERNEL

The conclusion of the preliminary study on the levitating layer was to simply use a refined grid to study very shallow beds with CFD-DEM. In this follow-up study, the validity of this recommendation is tested by simulating the same problem discussed in Section 2 with a grid of $\Delta^* = 1/3$. As mentioned in Section 4, fine grids with $\Delta^* < 1$ incur interpolation challenges. Specifically, the Square DPVM interpolation scheme used in Section 2, as implemented in MFiX, does not extend beyond one adjacent layer of cells. It is possible to extend the particle interpolation to more than one layer of adjacent cells, however this, in turn, would cause a bottleneck for distributed memory parallel (DMP) implementations. A more efficient method of particle-grid interpolation on fine grids is to deposit particle information directly on the grid which is then smoothed with a Gaussian kernel solving a diffusion equation (Capecelatro et al., 2013). Although an implementation of the diffusion kernel is available in MFiX Release 2016.1, a slightly modified version of the code[1] was used which includes variable (artificial) time stepping in the diffusion equation solver which improves numerical stability.

There still remains uncertainty in the width, δ_f^*, of the Gaussian filter which determines the length over which the fluid experiences the effects of a given particle. Here, $\delta_f^* = 1.5$ is selected for (some) consistency with the previous Square DPVM results. The high-resolution simulation fluidizes similar to the previous $\Delta^* = 1$ (Square DPVM) simulation. The pressure profile of the fine grid solution is compared to the previous Square DPVM solutions in Figure 3. Interestingly, the pressure profile does not show a minimum near the top of the bed. Instead, the gas-phase pressure smoothly decreases from the high-gradient "bed" region to the low-gradient freeboard region. The bed pressure drop previously predicted by the modest grids ($\Delta^* \leq 2$) is in good agreement with the fine grid solution.

---

[1] MFiX branch jm-4-wdf provided by Jordan Musser

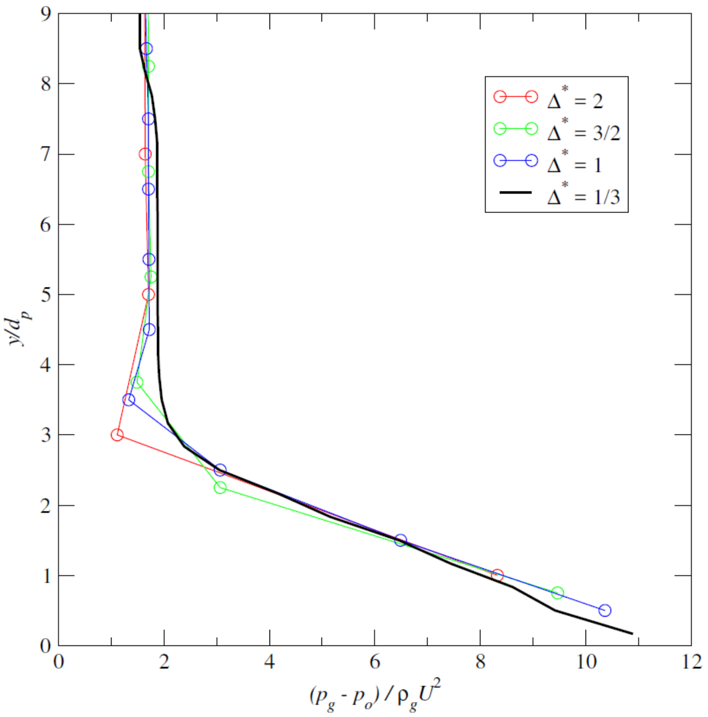

Figure 3: Gas-phase vertical pressure profile averaged over bed width and depth from *t* = 0.5 to 1 s including the high-resolution Gaussian kernel solution.

6. REFERENCES

Capecelatro, J.; Desjardins, O. An Euler-Lagrange strategy for simulating particle-laden flows. *Journal of Computational Physics* **2013,** *238*, 1–31.

Ding, J.; Gidaspow, D. A bubbling fluidization model using kinetic theory of granular flow. *AIChE Journal* **1990,** *36*, 523–538.

Garg, R.; Galvin, J.; Li, T.; Pannala, S. Documentation of open-source MFIX-DEM software for gas-solids flows; Technical Report; National Energy Technology Laboratory: Morgantown, WV, 2012a. https://mfix.netl.doe.gov/documentation/dem_doc_2012-1.pdf

Garg, R.; Galvin, J.; Li, T.; Pannala, S. Open-source MFIX-DEM software for gas-solids flows: Part I-Verification studies. *Powder Technology* **2012b,** *220*, 122–137.

Lathouwers, D.; Bellan, J. Modeling of dense gas-solid reactive mixtures applied to biomass pyrolysis in a fluidized bed. *International Journal of Multiphase Flow* **2001,** *27*, 2155–2187.

Waterson, N. P.; Deconinck, H. Design principles for bounded higher-order convection schemes - a unified approach. *Journal of Computational Physics* **2007,** *224*, 182–207.

Wen, C. Y.; Yu, Y. H. A generalised method for predicting minimum fluidization velocity. *AIChE Journal* **1966,** *12*, 610–612.

Sean Plasynski, Ph.D.
Director (Acting)
National Energy Technology Laboratory
U.S. Department of Energy

John Wimer
Associate Director
Strategic Planning
Science & Technology Strategic Plans
& Programs
National Energy Technology Laboratory
U.S. Department of Energy

Brian Morreale
Executive Director
Research & Innovation Center
National Energy Technology Laboratory
U.S. Department of Energy

NETL Technical Report Series